Archaeological and Anthropological Sciences (2022) 14:85
https://doi.org/10.1007/s12520-022-01501-w

ORIGINAL PAPER

Discrimination of wheel-thrown pottery surface treatment by Deep Learning

Josef Wilczek[1,2] · Richard Thér[1] · Fabrice Monna[2] · Christian Gentil[3] · Céline Roudet[3] · Carmela Chateau-Smith[4]

Received: 22 June 2021 / Accepted: 31 December 2021

Abstract

The study of pottery surface treatment is essential to understand techniques used by ancient potters, in order to explore the cultural and economic organisation of past societies. Pottery is one of the most abundant materials found in archaeological excavation, yet classification of pottery surface treatments remains challenging. The goal of this study is to propose a workflow to classify pottery surface treatments automatically, based on the extraction of images depicting surface geometry, calculated from 3D models. These images are then classified by Deep Learning. Three Convolutional Neural Network algorithms (VGG16 and VGG19 transfer learning, and a custom network) are quantitatively evaluated on an experimental dataset of 48 wheel-thrown vessels, created by a professional potter specifically for this study. To demonstrate workflow feasibility, six different surface treatments were applied to each vessel. Results obtained for all three classifiers (accuracy of 93 to 95%) surpass other state-of-the-art quantitative approaches proposed for pottery classification. The workflow is able to take into account the entire surface of the pottery, not only a pre-selected spatially limited area.

Keywords Archaeology · Automatic pottery classification · Surface treatment · Deep Learning · Experimental dataset

Introduction

Creating artefacts is an essential social activity and therefore a key topic for archaeological investigations. Pottery is among the most abundant of artefacts and is a medium of cultural information that provides valuable evidence of the chronology, economics, and development of past societies (Shepard 1956; Rye 1981; Orton et al. 1993; Renfrew and Bahn 2015). Manufacturing pottery often requires a complex sequence of tasks (*chaine operatoire*), which includes selection of raw materials, preparation of pottery paste, forming, and firing. The *chaine operatoire* is often investigated by means of ethnographic analogies or experimental archaeology (e.g. Martineau 2000; Gosselain 2002; Livingstone Smith 2007; Roux 2017a, 2017b, 2019).

The surface treatment of pottery is among the final set of actions in the forming stage of the *chaine operatoire*. It comprises the operations carried out after shaping and before firing (surface treatment in Gibson and Woods 1997, pp. 42–44; Santacreu 2014, pp. 82–86; surface finishing in Rice 2015, pp. 136–141). It is a set of actions transforming the inner and outer vessel surface by friction (e.g. softening, burnishing, shining, scratching, and grating) and/or coating (e.g. applying clay, graphite, carbon, or organic materials); it contributes greatly to the visual quality of the artefact, as well as to functional properties such as permeability, higher thermal conductivity, and general surface resistance (e.g. Kappel 1969; Hlava 2008; Pétrequin et al. 2009; Martineau 2010, 2013; Venclová et al. 2013; Roux 2017a, 2017b, 2019). Recent trends in pottery surface investigations concern identification of the tools and techniques used in pottery fabrication (e.g. Forte 2012; Manzaneda et al. 2018; Gawron-Szymczyk et al. 2020; Melis and Roselló 2021), determination of pottery function (Forte et al. 2018; Bajeot et al. 2020), study of pottery craft specialisation (Forte 2019), and

✉ Josef Wilczek
josef.wilczek@hotmail.com

1 Department of Archaeology, University of Hradec Králové, Rokitanského 62, 50003 Hradec Králové, Czech Republic

2 ARTEHIS, UMR CNRS 6298, Université Bourgogne–Franche Comté, 6 Boulevard Gabriel, Bat. Gabriel, 21000 Dijon, France

3 LIB, EA7534, Université Bourgogne–Franche Comté, 9 avenue Alain Savary, 21000 Dijon, France

4 CPTC, EA4178, Université de Bourgogne, 4 boulevard Gabriel, 21000 Dijon, France

Published online: 11 April 2022

phylogenetic analysis of the evolution of ceramic traditions (Manem 2020).

Researchers usually describe the topography of pottery surface treatment using qualitative categories observable by the naked eye, or by stereomicroscope at low magnification (e.g. Rye 1981, pp. 89–95; Binder et al. 1994; Gelbert 2003; Martineau and Maigrot 2004; Thér and Neumannová 2012; Lepère 2014; Rice 2015, pp. 137–141; Roux 2019, pp. 195–205). Results are then presented in the form of referential images. Classifications in archaeology depend not only on aspects related to the artefacts under study (e.g. period, origin, variability), but also on the methodology used (e.g. microscopic or macroscopic observation, paradigm), and even on the researcher's profile (e.g. level of expertise, specialisation, research history). These factors may sometimes lead to discrepancies in the definition and classification of the same phenomena observed by different researchers, and could perhaps limit the reproducibility of the results obtained (e.g. Hodson et al. 1966; Binford 1972; Adams and Adams 1991; Orton et al. 1993; Arnold 1999; Di Angelo et al. 2018; Cintas et al. 2020). Classifying the enormous quantity of artefacts discovered during excavation remains time-consuming, whatever the method used, so automating the classification process could provide helpful assistance for specialists working with pottery artefacts (e.g. Karasik and Smilansky 2011; Gualandi et al. 2016; Navarro et al. 2021).

In order to overcome these issues, many efforts have been made to develop solutions for automatic pottery retrieval and classification, based on quantitative data, such as vectorized drawings, digital photographs, or 3D models. However, these studies have focused almost exclusively on the shape of the pottery (e.g. Karasik and Smilansky 2011; Gualandi et al. 2016; Navarro et al. 2021; Wilczek et al. 2021), and to a lesser extent on other aspects, such as colour, paste, or decoration (e.g. Bickler 2018; Gualandi et al. 2021). The identification of the fabrication and use of an artefact based on various quantitative surface parameters has been extensively explored for bone (e.g. Legrand and Radi 2008; Emery 2009; Buc 2011), and for lithic artefacts (e.g. Stemp and Chung 2011; Stemp 2014; Evans et al. 2014; see Stemp et al. 2015 for a detailed literature review), but remains relatively rare in investigations of archaeological pottery (Díaz Bonilla 2019; Ionescu et al. 2019; Díaz Bonilla et al. 2020; Ionescu and Hoeck 2020). These innovative studies select zones of interest, identified by the specialist, for microscopic inspection. Examining the entire surface of the artefact in greater detail could help to provide a more global perspective on the treatments applied to the pottery surface during fabrication. Discrimination between surfaces is based on many parameters calculated from distances between the surface of the artefact and the plane passing through this surface (e.g. root mean square height of the surface, maximum height of peaks, maximum height of valleys; see ISO 25178 standards; ISO 2012; Blateyron 2013). As the archaeological pottery surface, at least at the macroscopic scale, is almost never flat, parameter calculation requires adapted pre-treatment.

Research aims Deep Learning (DL) is now increasingly used for classification purposes, in almost all scientific domains, including archaeology and cultural heritage (e.g. Wang et al. 2017; Cintas et al. 2020; Di Angelo et al. 2021; Garcia-Molsosa et al. 2021; Gualandi et al. 2021; Navarro et al. 2021). The aim of this article is to present and evaluate three DL methods for the automatic identification of pottery surface treatments. This workflow is based on the supervised classification of images depicting surface geometry of 3D models of pottery vessels. One custom and two state-of-the-art DL algorithms are evaluated on different surface treatments from an experimental dataset. This corpus was specifically created by a professional potter to test the workflow proposed in this study. The use of an experimental dataset rather than archaeological fragments allowed full control of the data and the classification results, thus demonstrating the feasibility of the approach proposed. The workflow presented here can easily be used by the archaeological community, whatever the corpus, in order to acquire new knowledge about past societies through the investigation of pottery surface treatments.

Material and methods

Test corpus

A test corpus of 48 vessels was created to validate the workflow for the automatic identification of surface treatments proposed in this study, using a commercially available fine-grained clay (Witgert company, production designation: 10 Steinzeugmasse rot). Half of the clay was tempered with alluvial sand (20%, grain size < 1 mm); the remaining half was tempered with crushed weathered mica schist (20%, grain size < 2 mm). To avoid introducing unnecessary variation by employing several experts, all vessels were produced by the same craftsman, a professional potter with over two decades of experience in pottery-forming techniques. All 48 vessels were wheel-thrown, with a simple conical shape (Fig. 1; approximate height 15 cm, rim diameter 16 cm, base diameter 7 cm).

The spectrum of surface treatments is derived from Late La Tène wheel-turned pottery found in Central Europe, where six basic types of texturing (Fig. 2), produced either by friction or by coating, have so far been identified (Venclová 1998, Fig. 54; Danielisová 2010, P4 Tab. 1). The two

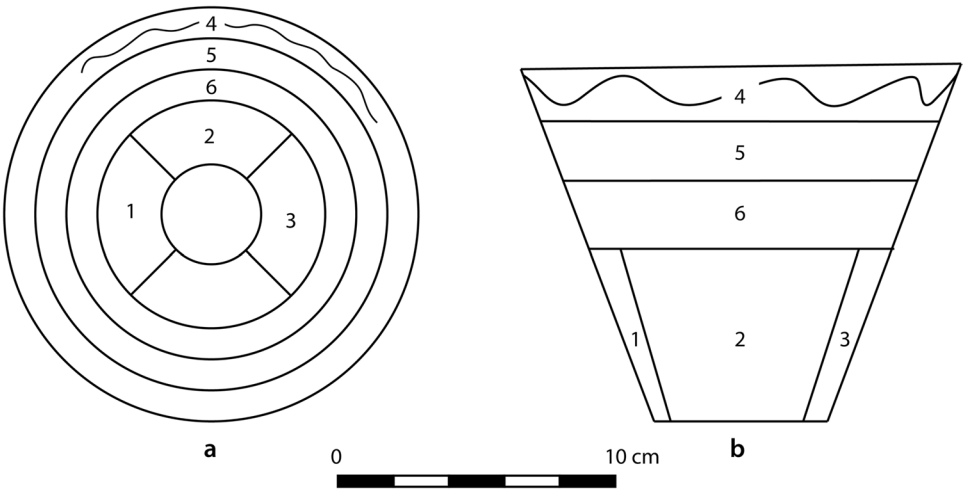

Fig. 1 Distribution of surface treatments on the vessel. (a) Bottom-up view. (b) Side view

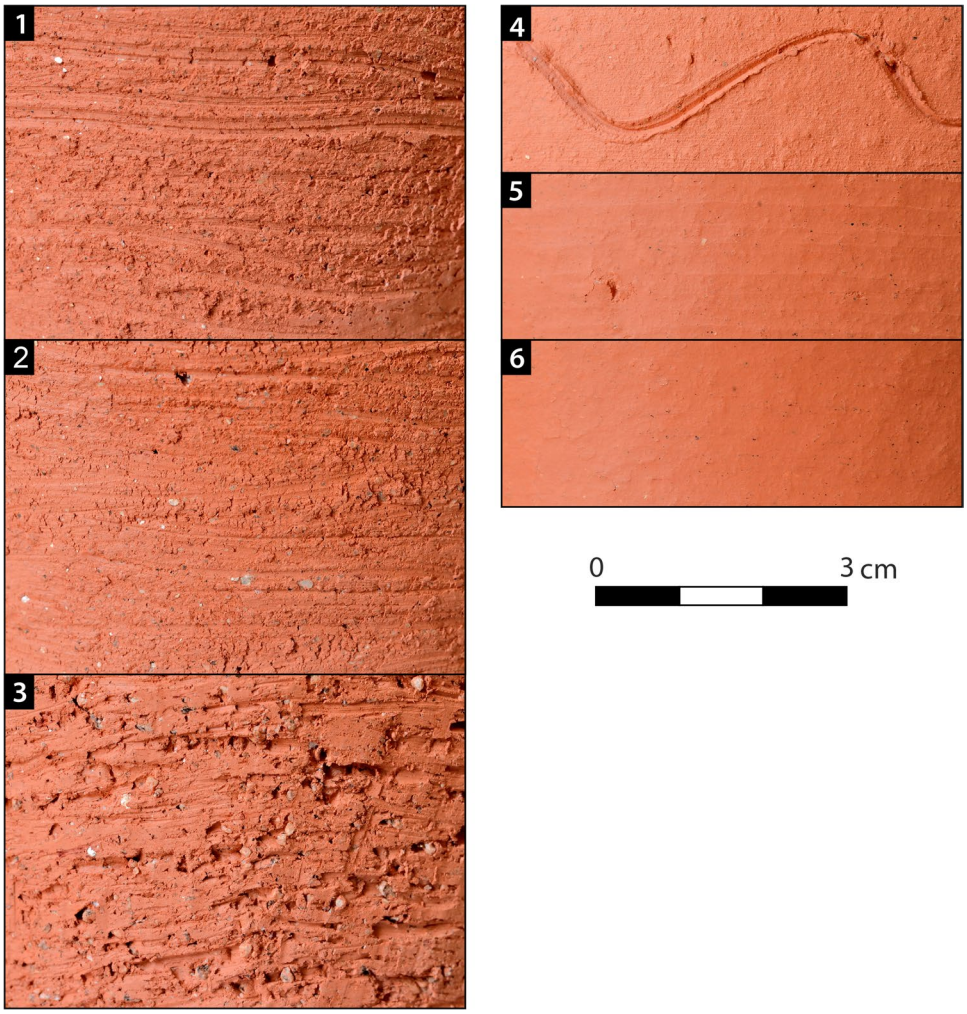

Fig. 2 Surface treatments after firing for the 6 zones analysed. See Table 1 for details

types of temper used in this study are also attested in La Tène pottery (Thér et al. 2015).

We limited the range of surface treatments used on the test corpus to those produced by friction. To introduce an outlying factor, a simple decorative technique was applied to each vessel (Table 1). To ensure vessel surface regularity before treatment, a blade was applied during the last stage of wheel-throwing.

Table 1 Description of surface treatments applied to each vessel. See Fig. 1 for details

Zone	Technique	State of drying	Approx. volume of water in the paste (in %)	Colour code for Figs. 3c, 7, and 8	Area (min, mean, max; in cm^2)	Classification of surface treatments of La Tène pottery (Venclová 1998, Fig. 54)
1	Dragging with coarse sandstone	Wet paste	30	Brown	41.9, 53.8, 68.5	Scratched
2	Dragging with coarse sandstone	Leather-hard	20	Red	43.4, 52.1, 62.8	Scratched
3	Scraping with blade	Leather-hard	20	Yellow	35.6, 51.9, 65.3	Grated
4	Wave engraved with wooden stick	Wet paste	30	Green	71.1, 126.4, 152.8	Grooved
5	Smoothing with agate pebble	Leather-hard		Cyan	89.8, 108.3, 132.5	Smoothed
6	Smoothing with agate pebble	Leather-hard	20	Blue	83.8, 100.5, 127.5	Burnished
	Burnishing with agate pebble	Nearly dry	15			

In the following descriptions, surface treatment classifications in italics correspond to those used by Venclová (1998, Fig. 54). To produce a similar effect to the *scratched* treatment on La Tène pottery (i.e. shallow, overlapping, irregular scratches), a coarse sandstone fragment (12 × 9.5 × 5 cm; see Supplementary Materials SM1) was dragged over the vessel. This procedure, using a rough-surfaced texturing tool, was applied at the wet paste stage (Zone 1), and at the leather-hard stage (Zone 2). The second treatment, corresponding to *grated*, was produced by scraping the surface with a blade. This technique leaves deep, sharply defined, irregular striations, produced as the blade displaces inclusions in the clay (Jansová 1964, p. 185). This procedure could only be applied at the leather-hard stage (Zone 3), as the force required to scrape the surface with a blade exceeds the strength of the vessel wall at the wet paste stage. To introduce a feature very different from the rest of the corpus, a zone with a decorative element (a continuous wave) was produced by engraving the surface with a wooden stick at the wet paste stage (Zone 4). To produce the treatments classified as *smoothed* and as *burnished*, a polished agate pebble (4 × 2.5 × 1.3 cm; see Supplementary Materials SM1) was rubbed over the surface (e.g. Skibo et al. 1997; Lepère 2014; Roux 2019). To produce a *smoothed* surface, the smoothing procedure was applied only once, at the leather-hard stage (Zone 5). To produce a *burnished* surface, the procedure was applied in two steps: first at the leather-hard stage, for smoothing, then at a more advanced stage (between leather-hard and completely dry), for burnishing (Zone 6).

The size of each surface treatment zone varied between 36 and 153 cm^2, with a mean area of 82 cm^2 (Table 1), which is considered sufficient for surface treatment analysis.

After surface treatment, all vessels were fired in an electric kiln in oxidising conditions up to 800 °C.

3D scanning and mesh segmentation

The experimental dataset (Fig. 3a) was scanned using an Artec Spider 3D scanning device with an accuracy of 0.05 mm, and a 3D resolution of 0.1 mm (Fig. 3b). Only the outer surface of the vessels was scanned, as the surface treatment was not applied to the inner surface. Each 3D model of a vessel was represented as a triangular mesh composed of 7.9 to 10.1 M vertices. Six zones, corresponding to the six different surface treatments (Table 1), were manually extracted from each 3D model, and labelled by the operator (Fig. 3c). A total of 288 meshes (i.e. 6 zones × 48 vessels) was thus obtained, each with 0.5 to 2.0 M vertices.

Model preparation

Pottery surface treatments can be identified by surface irregularity, which corresponds to geometric fluctuation in relation to a smooth reference surface. Pottery vessels are often roughly symmetrical around their rotational axis, which is the case for the simple conical vessels in the dataset. Several solutions exist for the identification of the optimal position of the rotational axis of archaeological pottery fragments, based on their 3D models (see e.g., Mara 2006; Karasik and Smilansky 2008; Wilczek et al. 2018, and references within). Ideally, the distances between the model surface and the cone approximating the vessel could be used as the pottery surface representation and thus as input in the analyses. However, archaeological pottery is usually not perfectly symmetrical and calculation of distances from the perfectly symmetrical shape would highlight the fragment's rotational asymmetry and any global deformation of the vessel rather than its local surface geometry (Mara 2009).

The local surface geometry of the vessels was therefore highlighted by calculating distances between the mesh and its smoothed version, obtained by application of the

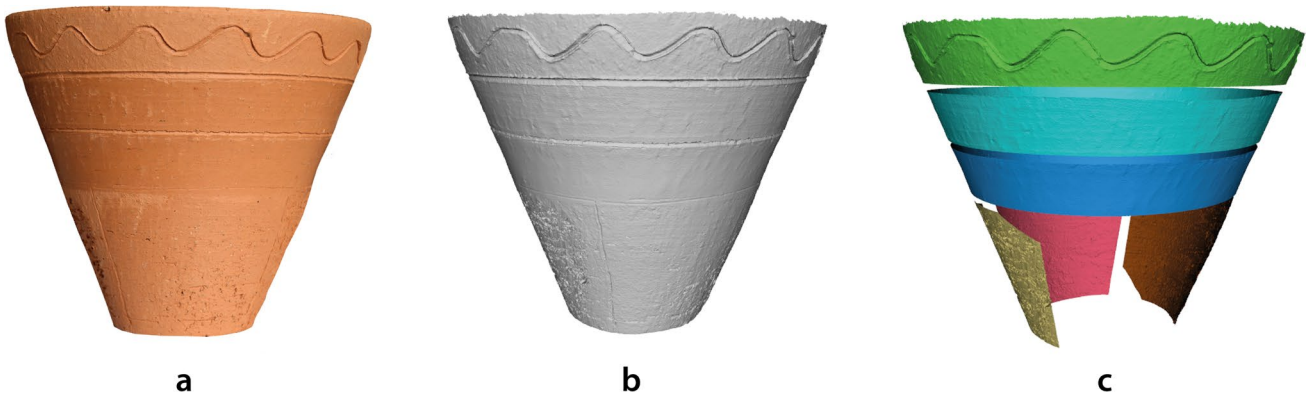

Fig. 3 Data acquisition and preparation. (a) Photograph of vessel. (b) 3D model of vessel. (c) 3D model manually segmented into 6 different surface treatment zones. For colour code, see Table 1. Note that the vessel is oriented 180° around the rotational axis in relation to Fig. 1b

Laplacian filter (99 iterations; Fig. 4a–c; Freitag 1997; Amenta et al. 1999). This filter suppresses high frequencies and is well adapted to meshes with non-uniform triangles. The distances expressed by different colours were then used as the texture of the 3D model (Fig. 4d). Colour representation was preferred to greyscale, as classification algorithms applied in the study use RGB images as inputs by default (see the "Deep Learning classification algorithms" section). The colour scheme applied here for visualisation of distances was chosen to maximise image information concerning deviation from the smoothed (reference) surface.

Image generation

A set of 240 randomly overlapping images was acquired from each mesh, by imitating the process of aerial orthophotography acquisition. Each image, taken perpendicularly to the surface, at 150 × 150 px resolution, with Field

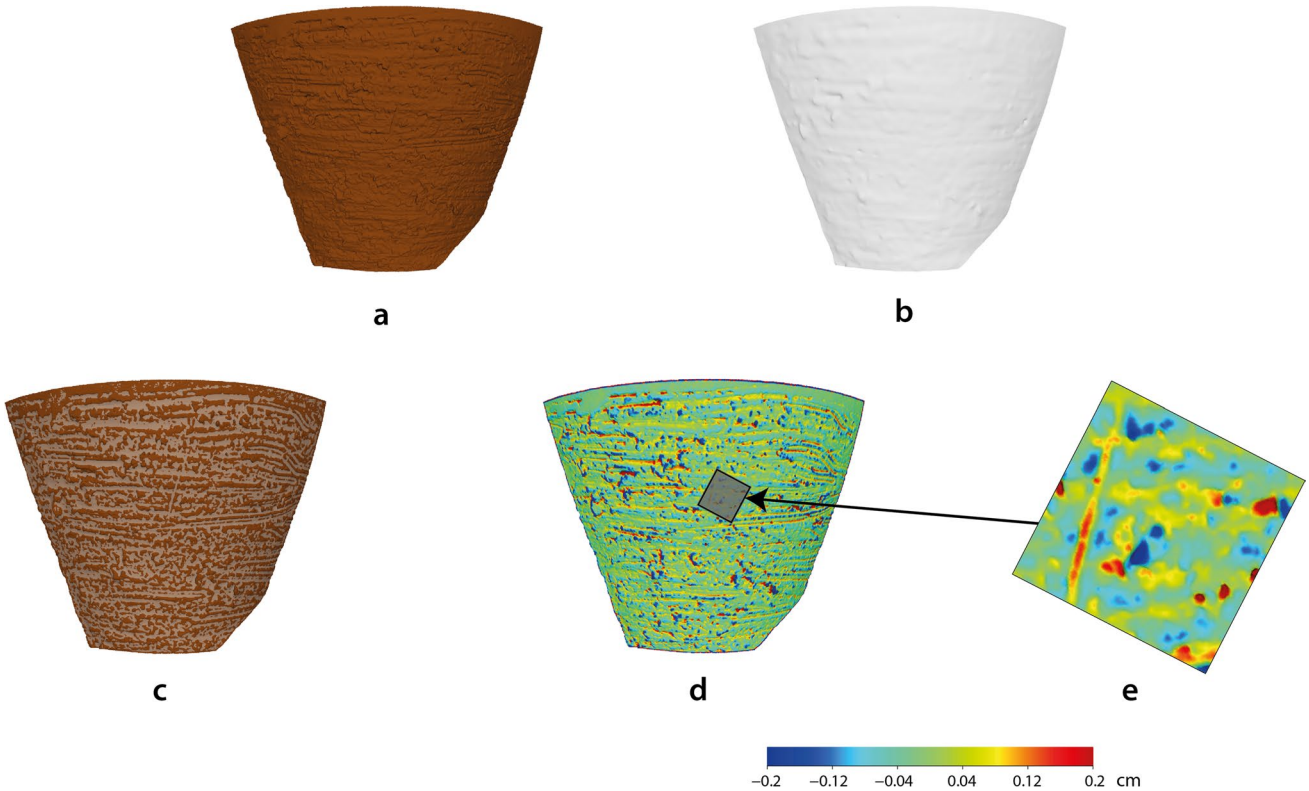

Fig. 4 Analysis of a given zone. (a) Mesh. (b) Smoothed version. (c) Superimposition of (a) and (b). (d) Distances between (a) and (b), expressed by a colour scale. (e) Extraction of an image perpendicular to the mesh surface, showing distances expressed by a colour scale

of View (FOV) set to 0, covered an area of approximately 1 cm^2 (Fig. 4e).

A total of 69,120 images (i.e. 288 meshes × 240 images) was generated by this process. Images with surface borders were then filtered out from the dataset, and the number of images within each surface treatment group was equalised. The final image dataset thus created contained 52,200 images (6 surface treatment groups, each composed of 8700 images).

Although acquiring images from 3D models may be less rapid than digital photography (e.g. Gualandi et al. 2021), images generated from 3D models should be less affected by variations in illumination, as the illumination model used to generate the 3D scene can be controlled (e.g. Nicodemus 1965; Gouraud 1971; Phong 1975). Images generated only from the surface geometry of the 3D model are not affected by the original colour of the fragment, which may be related to other factors (e.g. clay type, firing, and/or soil composition where the pottery was found).

Deep Learning classification algorithms

Deep Learning algorithms are based on Artificial Neural Networks (ANNs), which mimic the way in which the brain responds to sensory stimuli, by modelling the relationship between input and output signals. A typical artificial neuron can be represented as:

$$y(x) = f\left(\sum_{i=1}^{n} w_i x_i\right)$$

where n is the number of input variables x; w represents input variable weighting; $f(x)$ is the activation function, and $y(x)$ is the output variable.

In the case of image classification, inputs correspond to RGB channel values stored in the image array, and outputs are the labels of the desired class. The activation function is used for better adaptation of the signal to the mathematical characteristics of the network. The optimisation process then estimates the optimal weights to minimise differences between expected and observed outputs.

A Convolutional Neural Network (CNN) is generally used for image classification, and it usually contains three types of layers: convolutional, pooling, and fully connected. The lower levels of the CNN seek to reduce input data complexity by applying filters (convolutional layers), and by downsampling matrices (pooling layers). Fully connected layers learn a more abstract representation of the processed data, and are found in the upper levels of the network. Lower layers of CNN usually extract colour information and edges, while upper layers account for shape and texture. The final classification layer contains the loss function, which transforms the input data into the corresponding output (e.g. LeCun et al. 2015; Gu et al. 2017; Wang et al. 2020).

A CNN usually requires a considerable number of annotated images and an adequate amount of time for accurate training. To reduce calculation time, 'transfer learning' uses a model pre-trained on a huge image dataset (i.e. hundreds of labels and millions of images) for another image classification task, as such a model is considered to contain features general enough to be adapted to almost any dataset (Pan and Yang 2010). The transfer learning process has sometimes been found more effective than training the CNN model from scratch (Tajbakhsh et al. 2016). However, as each pre-trained CNN model is specific to a given classification task and to the dataset it was trained on, the final layers of this model need to be re-trained and fine-tuned on the new dataset, to integrate new images and classes (Yosinski et al. 2014).

Three CNN models were used to classify pottery surface treatment images. The first two models are among the most popular CNN models used for image classification: VGG-16 and VGG-19, developed by the Visual Geometry Group Lab, Oxford University (Simonyan and Zisserman 2015). The 13 (VGG-16) or 16 (VGG-19) convolutional layers are followed by 3 fully connected layers (Fig. 5a–b). The particularity of these models is that the convolutional layers use very small 3 × 3 filters, and the volume of data is reduced by 2 × 2 max-pooling layers. All hidden layers contain Rectified Linear Units (ReLUs; Krizhevsky et al. 2017). At the end of the model, two of the fully connected layers have 4096 nodes each, followed by the final softmax classifier (Gao and Pavel 2018). Both VGG-16 and VGG-19 were pre-trained on the ImageNet dataset, containing 1.4 M images and 1000 classes (Russakovsky et al. 2015). As the ImageNet dataset consists of images (e.g. dogs, cats, and cars) very different from those analysed in this study, the last three layers of the models were re-trained on the pottery surface treatment dataset. The third model was defined and trained from scratch. This rather simple Custom CNN model was composed of 4 convolutional layers, followed by 2 fully connected layers (Fig. 5c; Chollet and Allaire 2018; Ghatak 2019). As with the VGG architecture, the convolution layers use 3 × 3 filters and are reduced by 2 × 2 max-pooling layers. All hidden layers use ReLU activations, except the final classification layer, which uses softmax.

Image pre-processing and training

Image RGB channel values were standardised to [− 1,1]. To increase robustness and avoid overfitting, the diversity of the training dataset was augmented by applying several random transformations (i.e. rotation, shear, zoom, and horizontal flip). Table 2 shows the range of values selected: the higher range of the rotation parameter was

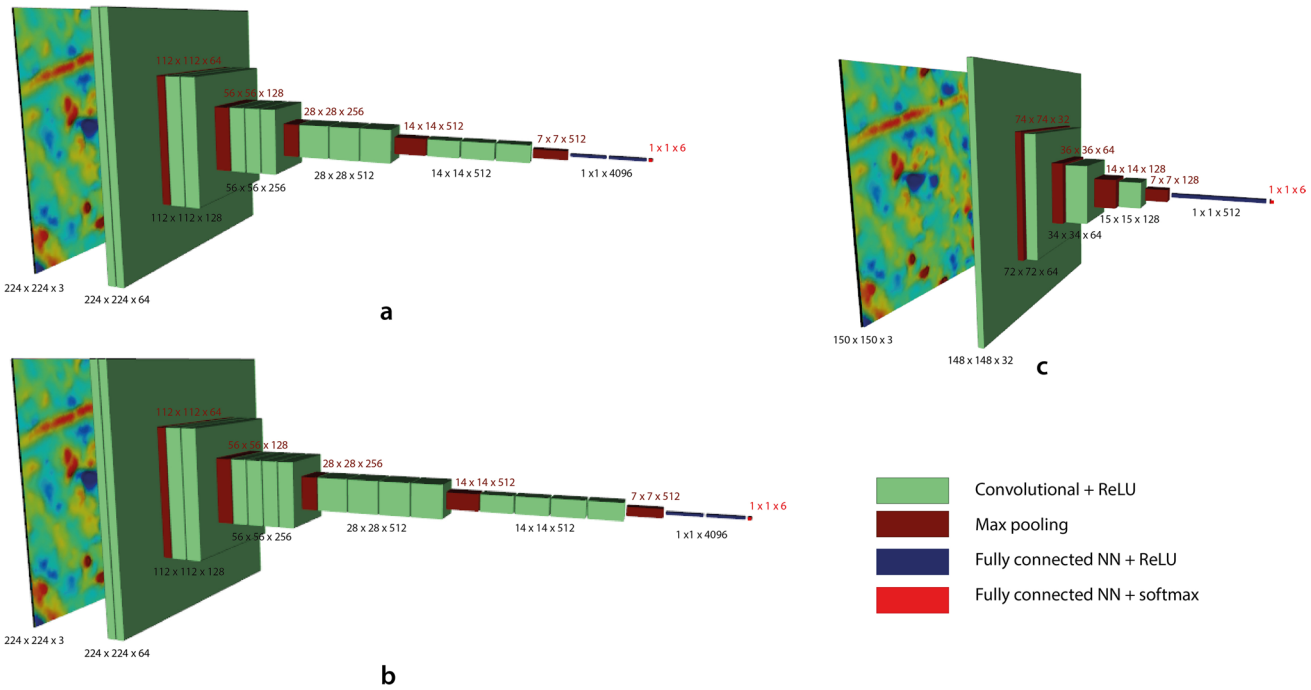

Fig. 5 Description of Deep Learning architectures. (a) VGG-16. (b) VGG-19. (c) Custom CNN

Table 2 Range of values selected for image augmentation in the training subset

Transformation	Rotation	Shear	Zoom	Horizontal flip
Range	[−90°, +90°]	[−0.2, +0.2]	[−0.2, +0.2]	[True, False]

chosen to take into account the fact that fragment orientation (i.e. its position according to the rotational axis) is considered to be unknown.

The dataset of 52,200 images, depicting 288 meshes, was randomly split into a training subset containing 36,540 images (70%), a validation subset of 10,440 images (20%), and a testing subset of 5220 images (10%).

Four commonly used optimisers, Adam (Kingma and Ba 2017), Adadelta (Zeiler 2012), Adamax (Kingma and Ba 2017), and Stochastic Gradient Descent (SDG; Ruder 2017), and four dropout regularisations (0, 0.1, 0.3, and 0.5) were tested on the dataset to identify the optimal combination of (i) optimisation method, allowing accurate estimation of weights in deep networks, and (ii) regularisation, to prevent overfitting. All models were trained for 50 epochs with the image batch size set to 32. Performance scores were evaluated on accuracy, defined as the ratio of correct predictions over the total number of images.

Classification visualisation

The procedure can classify each vertex on the 3D model surface based on the class of the image in which the vertex is visible. When the vertex is visible in multiple images classified in different groups, the class of the vertex can be given by majority voting, i.e. based on the most frequent class of images containing the vertex. This procedure can also highlight, or omit, vertices that cannot be classified unambiguously, e.g. those for which the frequencies of votes for different classes are almost equal.

Software and hardware

The Artec Studio Professional software (version 15) was used for 3D mesh production. The Meshlab software (Cignoni et al. 2008) was used for model segmentation. Surface treatment images were generated by a script encoded in the R programming language (R Core Team 2021), using the 'rgl' (Adler and Murdoch 2021) and 'Rvcg' (Schlager 2017) libraries. Supervised classification was produced in Python (Python Software Foundation 2021), with the 'numpy' (Harris et al. 2020), 'pandas' (McKinney 2010), 'keras' (Chollet et al. 2021), and 'tensorFlow' (Abadi et al. 2016) libraries. A consumer-grade computer (Intel Core i7-4712HQ—2.50 GHz, 16 Go DDR3, NVIDIA GeForce GTX 980 M) was used for calculations.

Results and discussion

Classification evaluation

The classification accuracy of DL models applied to the test dataset varied between 83.3 and 94.5%, depending on the choice of optimiser and dropout value (Table 3). The best results for each DL model were obtained using the Adamax or SGD optimisers with little or no dropout regularisation. The pre-trained VGG19 yielded the best performance, followed by VGG16, and Custom CNN. After tuning, the very slight difference in accuracy (ranging from 93.4 to 94.5%) suggests that all three models are suitable classifiers, but also that the dataset and procedure are fit for purpose, and well able to answer the question of surface treatment classification. Each surface treatment (*scratched* (wet paste), *scratched* (leather-hard), *grated*, *grooved*, *smoothed*, *burnished*; see Table 1) has its own clearly identifiable geometry (Fig. 2). Although VGG16 and VGG19 present a slight gain in precision, Custom CNN achieves faster learning, as the number of parameters to be estimated is approximately 44 times smaller (see also Table 4). It should be noted that each classification model will produce slightly different classification outputs. Examining outputs both visually and quantitatively for each classification may prove to be the optimal solution.

Classification performance is similar to that obtained for the shape classification of pottery vessels into several groups (Table 5), or for the pixelwise binary classification of archaeological structures based on images obtained by drone, which was an easier task (Monna et al. 2020). The classification performance is similar to that based on the statistical treatment of a set of 30 surface parameters calculated from raster images of experimental samples obtained by laserscanning confocal microscopy (Díaz Bonilla et al. 2020). Representing the distance of the mesh from its smoothed version, encoded as RGB images, may thus be considered to provide useful information for surface treatment differentiation. It should therefore be possible, if and when required, to supplement or complement the more precise but more costly and more local microscopic approach with the workflow presented here.

An example of classification output can be seen in Table 6, showing very little overlap between zones. Fewer than 250 out of 5220 cases (i.e. only 4.7% of cases) were misclassified, due to occasional confusion between zones where identical techniques were applied: Zones 1 and 2 (*scratched* surface treatment) both used coarse sandstone dragging, but at different drying stages; Zone 5 (*smoothed*) and Zone 6 (*burnished*) both used agate rubbing, but at different drying stages. Such cases can usually be distinguished by the expert in a given pottery assemblage, but it is often difficult and time-consuming to transfer this expertise to a different dataset. Macroscopic observations confirm that very similar traces are sometimes found on meshes representing different surface treatments (Fig. 6: A1, A2, B1, B2). Another potential cause of misclassification is the great variety of traces for a given type of surface treatment (Fig. 6: A3, B3; see Supplementary Materials SM2 for more examples). These recurring issues are intrinsic to all approaches seeking to classify or differentiate between real-world phenomena, such as archaeological pottery surface treatments. While the researcher will often focus on a specific descriptor and zone to differentiate between surface treatments, DL algorithms

Table 3 Comparison of surface detection accuracy on the test subset, using 3 Deep Learning algorithms (in %). The mean accuracy and standard deviation (shown in parentheses) were calculated from the last 10 epochs. The highest mean accuracy for each model-optimiser pair is highlighted in bold. The highest mean accuracy for each model-optimiser-dropout triplet is highlighted in bold italic. *D* dropout, *SGD* Stochastic Gradient Descent

Model	Optimiser	$D=0.0$	$D=0.1$	$D=0.3$	$D=0.5$
Custom CNN	Adam	91.8 (0.9)	**92.4** (0.6)	90.8 (1.0)	91.3 (0.7)
	Adadelta	**85.1** (0.3)	83.3 (0.4)	83.7 (0.2)	83.9 (0.3)
	Adamax	***93.4*** (0.6)	93.2 (0.5)	92.7 (0.8)	92.5 (0.9)
	SGD	89.4 (0.7)	90.1 (1.0)	89.5 (1.7)	**90.2** (0.9)
VGG16	Adam	**92.2** (1.3)	91.2 (1.3)	91.6 (1.3)	87.5 (2.5)
	Adadelta	92.9 (1.1)	**93.1** (0.8)	92.7 (0.7)	**93.1** (0.9)
	Adamax	92.7 (1.4)	***93.7*** (0.7)	93.1 (1.0)	93.1 (1.3)
	SGD	92.4 (1.7)	92.8 (1.7)	92.9 (1.1)	**93.1** (0.9)
VGG19	Adam	**91.8** (1.6)	90.3 (1.8)	88.8 (2.8)	88.0 (1.3)
	Adadelta	92.3 (1.5)	92.6 (1.4)	**92.7** (0.7)	92.3 (0.5)
	Adamax	**93.2** (1.2)	**93.2** (1.4)	92.5 (1.3)	93.0 (0.8)
	SGD	93.7 (1.5)	***94.5*** (0.9)	93.9 (0.7)	93.3 (1.9)

Table 4 Overview of the algorithms used for the automatic classification of pottery surface treatments

Model	Number of layers (convolutional / fully connected / total)	Total number of parameters	Trainable parameters	Image input size
Custom CNN	4 / 2 / 6	3,455,686	3,455,686	150×150
VGG16	13 / 3 / 16	138,357,544	130,722,280	224×224
VGG19	16 / 3 / 19	143,667,240	133,082,088	224×224

Table 5 Comparison with the literature. Abbreviations: *CNN* Convolutional Neural Network. Note that Top3 and Top5 accuracy is not given for this study, as prediction is based on a smaller number of classes

Classification applied to	Data	Methods	Number of samples	Classes	Accuracy (%) Top1/Top3/Top5	Reference
Surface treatment	Raster images	CNN	52,200	6	93–95/-/-	This study
Surface treatment	Raster images obtained by laser-scanning confocal microscopy	Discriminant analysis calculated on 30 surface parameters	240	6	85/-/-	Díaz Bonilla et al. (2020)
Decoration	Raster images	CNN (transfer learning using ResNet-50)	8000 augmentation to 100,000	65	-/-/77–84	Gualandi et al. (2021)
Pottery fragments based on shape	Profile coordinates	CNN (PointNet derivative, PointNet + +, PointCNN)	435 + 240 (?)	65	70–80/-/- (synthetic data) 2–22/-/8–58 (real-world data)	
Pottery rim fragments based on shape	Profile coordinates	Iterative Closest Point	319	14	82/93/96	Wilczek et al. (2021)
Complete vessels based on shape	Profile coordinates	Ramer-Douglas-Peucker polyline	1133	11	87/98/99	Lucena et al. (2016)
Complete vessels based on shape	Raster images	CNN	1133	11	90/-/-	Cintas et al. (2020)
Complete vessels based on shape	Raster images Profile coordinates	CNN (transfer learning using ResNet-18)	1282	11	96/-/-	Navarro et al. (2021)

Table 6 Confusion matrix (see Table 3 for model triplet details). Correctly classified samples are highlighted in bold

		Observed (classified by VGG19-SGD-D0)					
	Zone	**1**	**2**	**3**	**4**	**5**	**6**
Expected (original)	**1**	**793**	77				
	2	76	**794**				
	3		4	**866**			
	4				**870**		
	5			1	3	**781**	85
	6					4	**866**

identify a variety of features from the images under analysis (here, several thousands of images).

Classification visualisation

An example of classification based on majority voting can be seen in Fig. 7. In practice, the specialist would naturally seek to classify only areas or surfaces classified by the model as a homogenous surface treatment. Most surfaces are very well predicted: the surface treatment class corresponds to the original class of the mesh (Fig. 7a). Surfaces for which the procedure proposes several different classes can easily be identified (e.g. Figure 7b: A2, A5, D1, E1), and may then be more closely inspected by the specialist.

Classification error can be minimised by setting the minimum probability value, α, above which the image is considered to be classifiable. By default, the image is automatically attributed to a class based on the highest probability value. In an ideal situation, this choice can increase the accuracy of the output (e.g. Candila and Palazzo 2020; Wilczek et al. 2021). Table 7 shows the percentage of classifiable vertices, and the accuracy of attribution, with increasing α values. For example, with a probability of $\alpha = 0.95$, approximately 83% of vertices can be classified, with very high accuracy (here, 99.0%). Visual inspection of classification outputs obtained with higher α values indicates that incorrectly classified vertices are often filtered out (Fig. 8). Tuning the α value can thus help a specialist to improve classification output in other situations.

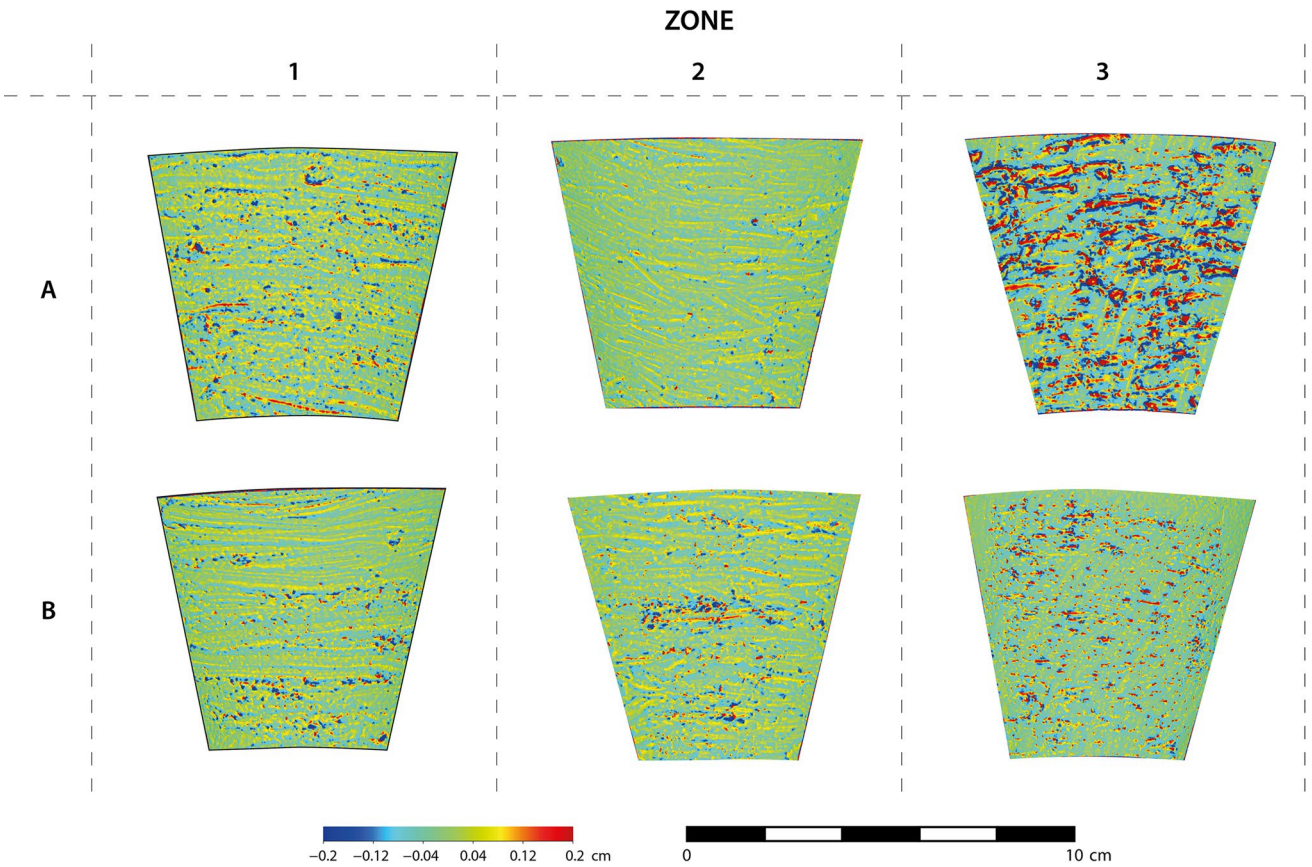

Fig. 6 Examples of meshes, showing distances between the mesh and its smoothed version represented by a colour scale (see Fig. 4 for details). Zones 1, 2, and 3 indicate surface treatments (see Table 1 for details). See Supplementary Materials SM2 for more examples

The high level of classification accuracy indicates that the DL algorithms learned to recognise 'the hand of the potter' who crafted the experimental dataset. It would be tempting to apply this classification approach directly to archaeological pottery fragments, but a classification model cannot be expected to identify surface treatments that it has never encountered. The surface treatment traces produced for this study by a professional potter did not reproduce all the techniques used to craft ancient pottery artefacts. Furthermore, the classification models tested here were trained on a dataset containing simple conical shapes, with no attempt to represent all the possible forms that exist among ancient pottery artefacts. Classifying the broad spectrum of ancient pottery production would require a much larger dataset, specifically tuned and adapted to the research question.

Concluding remarks

The goal of this pilot study was to show the feasibility of the DL approach. The procedures explored here map out a workflow that can be adapted to a broad variety of archaeological contexts: for example by working directly with a corpus of pre-annotated ancient fragments. The experimental dataset itself could also be expanded by adding more vessels, by increasing shape variability, and by integrating vessels crafted by other potters, to introduce more variability in surface treatment traces. Although the workflow was tested on wheel-thrown pottery, it should also be suitable for use with hand-made production.

Digital imaging and artificial intelligence are dynamic domains providing powerful solutions for classification in many scientific fields. To classify pottery surface treatments, this study evaluated three Deep Learning algorithms, two of which are based on transfer learning. All three methods yielded very good results (93–95% accuracy for a classification with 6 groups), among the highest scores so far achieved for classification problems related to archaeological pottery investigations. Classification accuracy can be further increased by taking into consideration only surfaces with high classifiability, thus opting for confidence over quantity. This fact may provide a practical solution for the routine work of surface treatment classification. Results obtained by such procedures may provide reliable guidance for surface identification, and may be used as a complement to the visual expertise of the specialist in the interpretation of traces.

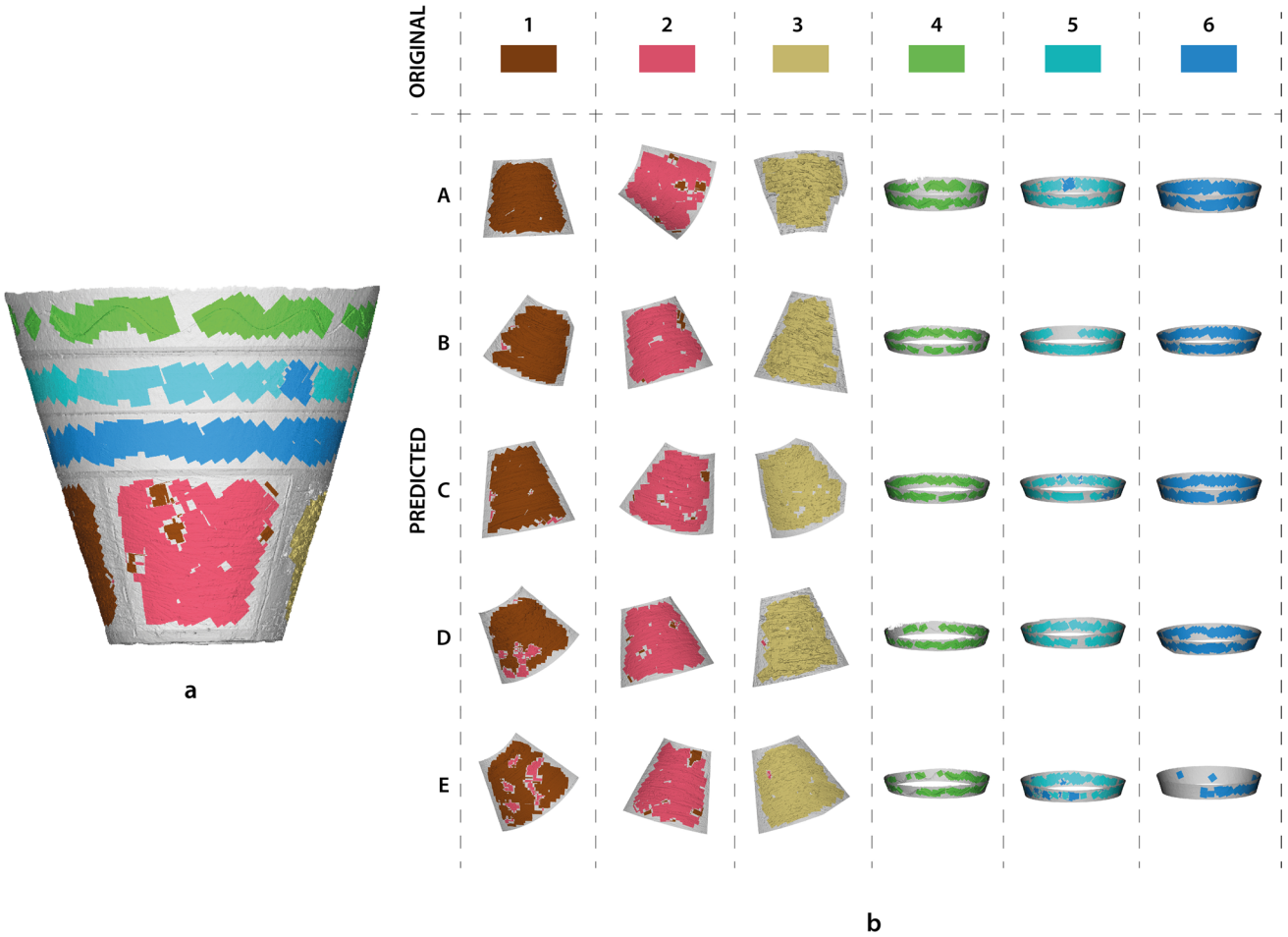

Fig. 7 Examples of visual outputs for the classification of surface treatments obtained with VGG19-SGD-D0. (a) Complete vessel colour-coded by surface treatment. (b) Meshes corresponding to surface treatment zones colour-coded by surface treatment. When the predicted surface possesses the same colour (i.e. class) as the original, the classification is correct. See Table 1 and Fig. 1 for details

Table 7 Classification of vertices based on minimum probability value (α). The VGG19-SGD-0 classification model was used here. Vertices were judged classifiable only if the probability of image classification was higher than α. Accuracy indicates the percentage of vertices judged classifiable that were attributed to the correct group

α	0.50	0.60	0.70	0.80	0.90	0.95	0.99
Classifiable (%)	100.0	98.0	96.8	92.8	87.7	83.4	70.9
Accuracy (%)	95.2	96.0	96.8	97.6	98.4	99.0	99.7

One of the advantages of the workflow presented here is that it can analyse the entire surface of the vessel. By expanding the focus of the analysis, previously overlooked elements can be brought to light. Analysing a broader surface makes quantification more reliable, possibly leading to the identification of specific techniques used or shared by a potter, a workshop, a household, or a community. The method of visualisation proposed here may facilitate the sharing of ideas and strategies with respect to classification among the broader archaeological community. Here, classification used images that measured approximately 1 cm^2. Although meaningful results were obtained at this resolution, the workflow can easily be adapted to classify features at any other macro- or microscopic scale. Although applied here for the classification of surface treatment, the same approach can also be used to classify other aspects of pottery (clay, decoration, etc.), and other archaeological artefacts

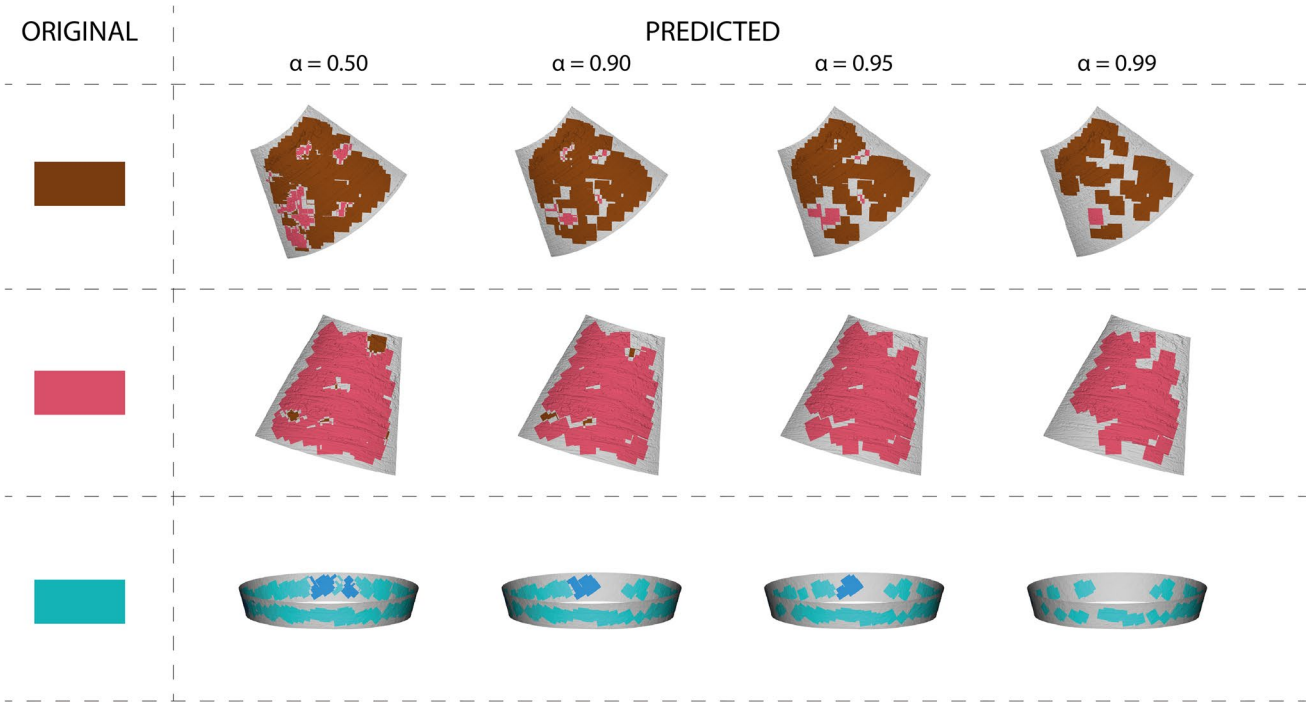

Fig. 8 Examples of classification of meshes based on different minimum probability values, α, for vertex classification. The VGG19-SGD-D0 classification model was used here

(weapons, tools, jewellery, etc.), based on the surface geometry of 3D models.

All the approaches presented here are easily reproducible by freely available software and/or packages (e.g. R, Python, Keras, TensorFlow), which can be adapted for routine use by archaeologists. The dataset of labelled images used for classification is made available to the broader scientific community via Github (https://github.com/jwilczek-dotcom) for further testing and benchmark comparison.

Supplementary Information The online version contains supplementary material available at https://doi.org/10.1007/s12520-022-01501-w.

Acknowledgements This article was produced within the scope of an Internation Research Team (IRT) project "Automatic extraction and interpretation of the formation of archaeologic pottery" supported by a grant from the Philosophical Faculty of the University of Hradec Králové. We are very grateful to the editor and the two anonymous reviewers whose pertinent and helpful comments have greatly improved the manuscript.

Data Availability Data are deposited in a repository.

Code availability Not applicable.

Declarations

Conflict of interest The authors declare no competing interests.

References

Abadi M, Barham P, Chen J, Chen Z, Davis A, Dean J, Devin M, Ghemawat S, Irving G, Isard M, Kudlur M, Levenberg J, Monga R, Moore S, Murray DG, Steiner B, Tucker P, Vasudevan V, Warden P, Wicke M, Yu Y, Zheng X (2016) Tensorflow: a system for large-scale machine learning. In: Proceedings of the 12th USENIX Symposium on Operating Systems Design and Implementation (OSDI '16), pp 265–283.

Adams WY, Adams EW (1991) Archaeological typology and practical reality: a dialectical approach to artifact classification and sorting. Cambridge University Press, Cambridge.

Adler D, Murdoch D (2021) rgl: 3D visualization using OpenGL. R package version 0.105.22. https://CRAN.R-project.org/package=rgl

Amenta N, Bern M, Eppstein D (1999) Optimal point placement for mesh smoothing. J Algorithms 30:302–322. https://doi.org/10.1006/jagm.1998.0984

Arnold PJI (1999) On typologies, selection, and ethnoarchaeology in ceramic production studies. In: Chilton ES (ed) Material meanings - critical approaches to the interpretation of material culture. The University of Utah Press, Salt Lake City, pp 103–117.

Bajeot J, Caricola I, Medeghini L, Vinciguerra V, Forte V (2020) An integrated approach based on archaeometry, use-wear analysis and experimental archaeology to investigate the function of a specific type of basin diffused in the Predynastic sites of lower Egypt (4th mill. BC). Quatern Int 555:135–149. https://doi.org/10.1016/j.quaint.2020.03.023

Bickler SH (2018) Machine learning identification and classification of histroic ceramics. Archaeol N Z 61:21–33.

Binford LR (1972) An archaeological perspective. Seminar Press, New York and London

Binder D, Gassin B, Sénépart I (1994) Éléments pour la caractérisation des productions céramiques néolithiques dans le sud de la France : l'exemple de Giribaldi (Complexe culturel du Chasséen méridional). In: Binder D, Courtin J (eds) Terre Cuite et Société. XIV Rencontres Internationales d'Archéologie et d'Histoire d'Antibes, APDCA, Juan-Les-Pins (1994). APDCA, Juan-les-Pins, pp 255–267.

Blateyron F (2013) The areal field parameters. In: Leach R (ed) Characterisation of areal surface texture. Springer Berlin Heidelberg, Berlin, Heidelberg, pp 15–43. https://doi.org/10.1007/978-3-642-36458-7_2

Buc N (2011) Experimental series and use-wear in bone tools. J Archaeol Sci 38:546–557. https://doi.org/10.1016/j.jas.2010.10.009

Candila V, Palazzo L (2020) Neural networks and betting strategies for tennis. Risks 8:68. https://doi.org/10.3390/risks8030068

Chollet F & others (2021) Keras. https://github.com/keras-team/keras

Chollet F, Allaire JJ (2018) Deep learning with R. Manning Publications.

Cignoni P, Callieri M, Corsini M, Dellepiane M, Ganovelli F, Ranzuglia G (2008) MeshLab: an open-source mesh processing tool. In: Scrano V, De Chiara R, Erra U (eds) Eurographics Italian Chapter Conference (2008). https://doi.org/10.2312/LOCALCHAPTEREVENTS/ITALCHAP/ITALIANCHAPCONF2008/129-136

Cintas C, Lucena M, Fuertes JM, Delrieux C, Navarro P, González-José R, Molinos M (2020) Automatic feature extraction and classification of Iberian ceramics based on deep convolutional networks. J Cult Herit 41:106–112. https://doi.org/10.1016/j.culher.2019.06.005

Danielisová A (2010) Oppidum České Lhotice a jeho sídelní zázemí. Archeologické studijní materiály 17. Archeologický ústav AV ČR, Praha.

Di Angelo L, Di Stefano P, Guardiani E, Morabito AE (2021) A 3D informational database for automatic archiving of archaeological pottery finds. Sensors 21:978. https://doi.org/10.3390/s21030978

Di Angelo L, Di Stefano P, Pane C (2018) An automatic method for pottery fragments analysis. Measurement 128:138–148.

Díaz-Bonilla S (2019) Experimentación aplicada a la cerámica prehistórica hecha a mano: creación de una colección experimental de referencia para el análisis del tratamiento de superficie. Treballs D'arqueologia 23:203–222.

Díaz Bonilla S, Mazzucco N, Gassiot Ballbè E, Clop García X, Clemente Conte I, Benavides Ribes A (2020) Approaching surface treatment in prehistoric pottery: exploring variability in tool traces on pottery surfaces through experimentation. Quatern Int 569–570:135–149. https://doi.org/10.1016/j.quaint.2020.06.027

Emery KF (2009) Perspectives on ancient Maya bone crafting from a Classic period bone-artifact manufacturing assemblage. J Anthropol Archaeol 28:458–470. https://doi.org/10.1016/j.jaa.2009.07.003

Evans AA, Lerner H, Macdonald DA, Stemp WJ, Anderson PC (2014) Standardization, calibration and innovation: a special issue on lithic microwear method. J Archaeol Sci 48:1–4. https://doi.org/10.1016/j.jas.2014.03.002

Forte V (2012) Investigating pottery technological patterns through macrowear analysis: the chalcolithic village of Maccarese-Fiumicino (Italy). International Conference on Use-Wear Analysis: Use-Wear 2012. Cambridge Scholars Publishing, Cambridge, pp 619–629.

Forte V (2019) Skilled people or specialists? Knowledge and expertise in copper age vessels from central Italy. J Anthropol Archaeol 55:101072. https://doi.org/10.1016/j.jaa.2019.101072

Forte V, Nunziante Cesaro S, Medeghini L (2018) Cooking traces on Copper Age pottery from central Italy: an integrated approach comprising use wear analysis, spectroscopic analysis and experimental archaeology. J Archaeol Sci Rep 18:121–138. https://doi.org/10.1016/j.jasrep.2017.12.052

Freitag LA (1997) On combining Laplacian and optimization-based mesh smoothing techniques. In: Trends in unstructured mesh generation, pp 37–43.

Gao B, Pavel L (2018) On the properties of the softmax function with application in game theory and reinforcement learning. https://arxiv.org/abs/1704.00805

Garcia-Molsosa A, Orengo HA, Lawrence D, Philip G, Hopper K, Petrie CA (2021) Potential of deep learning segmentation for the extraction of archaeological features from historical map series. Archaeol Prospect 28:187–199. https://doi.org/10.1002/arp.1807

Gawron-Szymczyk A, Łaciak D, Baron J (2020) To smooth or not to smooth? A traceological and experimental approach to surface processing of Bronze and Iron Age ceramics. Sprawozdania Archeologiczne 72. https://doi.org/10.23858/SA/72.2020.2.2275

Gelbert A (2003) Traditions céramiques et emprunts techniques dans la vallée du fleuve Sénégal. Maison des sciences de l'homme : Epistèmes, Paris.

Ghatak A (2019) Deep Learning with R. Springer, Singapore. https://doi.org/10.1007/978-981-13-5850-0

Gibson AM, Woods A (1997) Prehistoric pottery for archaeologist. Leicester University Press, Leicester.

Gosselain O (2002) Poteries du Cameroun meridional. Styles techniques et rapports à l'identité. CNRS, Paris.

Gouraud H (1971) Continuous shading of curved surfaces. IEEE Trans Comput 20:87–93.

Gu J, Wang Z, Kuen J, Ma L, Shahroudy A, Shuai B, Liu T, Wang X, Wang L, Wang G, Cai J, Chen T (2017) Recent advances in convolutional neural networks. https://arxiv.org/abs/1512.07108

Gualandi ML, Gattiglia G, Anichini F (2021) An open system for collection and automatic recognition of pottery through neural network algorithms. Heritage 4:140–159. https://doi.org/10.3390/heritage4010008

Gualandi ML, Scopigno R, Wolf L, Richards J, Buxeda i Garrigos J, Heinzelmann M, Hervas MA, Vila L, Zallocco M (2016) ArchAIDE Archaeological Automatic Interpretation and Documentation of cEramics. In: Catalano CE, De Luca L (eds) EUROGRAPHICS Workshop on Graphics and Cultural Heritage (2016). Eurograph Assoc pp 203–206. https://doi.org/10.2312/gch.20161408

Harris CR, Millman KJ, van der Walt SJ, Gommers R, Virtanen P, Cournapeau D, Wieser E, Taylor J, Berg S, Smith NJ, Kern R, Picus M, Hoyer S, van Kerkwijk MH, Brett M, Haldane A, del Río JF, Wiebe M, Peterson P, Gérard-Marchant P, Sheppard K, Reddy T, Weckesser W, Abbasi H, Gohlke C, Oliphant TE (2020) Array programming with NumPy. Nature 585:357–362. https://doi.org/10.1038/s41586-020-2649-2

Hlava M (2008) Grafit v době laténské na Moravě (Grafit in der Latènezeit in Mähren). Památky Archeologické 99:189–258.

Hodson FR, Sheath PHA, Doran JE (1966) Some experiments in the numerical analysis of archaeological data. Biometrika 53:311–324.

Ionescu C, Fischer C, Hoeck V, Lüttge A (2019) Discrimination of ceramic surface finishing by vertical scanning interferometry: discrimination of ceramic surface finishing by VSI. Archaeometry 61:31–42. https://doi.org/10.1111/arcm.12410

Ionescu C, Hoeck V (2020) Ceramic technology. How to investigate surface finishing. Archaeological and Anthropological Sciences 12, 204. https://doi.org/10.1007/s12520-020-01144-9

ISO (2012) ISO 25178–2:2012 Geometrical product specifications (GPS) — surface texture: areal — part 2: terms, definitions and surface texture parameters. https://www.iso.org/standard/42785.html

Jansová L (1964) Svědectví keramiky o pobytu Bojů na jihozápadním Slovensku a v přilehlém území. Studijní Zvesti AU SAV 13:185–194.
Kappel I (1969) Die Graphittonkeramik von Manching. Die Ausgrabungen in Manching – Band 2. Stuttgart.
Karasik A, Smilansky U (2008) 3D scanning technology as a standard archaeological tool for pottery analysis: practice and theory. J Archaeol Sci 35:1148–1168. https://doi.org/10.1016/j.jas.2007.08.008
Karasik A, Smilansky U (2011) Computerized morphological classification of ceramics. J Archaeol Sci 38:2644–2657. https://doi.org/10.1016/j.jas.2011.05.023
Kingma DP, Ba J (2017) Adam: a method for stochastic optimization. http://arxiv.org/abs/1412.6980
Krizhevsky A, Sutskever I, Hinton GE (2017) ImageNet classification with deep convolutional neural networks. Commun ACM 60:84–90. https://doi.org/10.1145/3065386
LeCun Y, Bengio Y, Hinton G (2015) Deep learning. Nature 521:436–444. https://doi.org/10.1038/nature14539
Legrand A, Radi G (2008) Manufacture and use of bone points from early Neolithic Colle Santo Stefano, Abruzzo, Italy. J Field Archaeol 33:305–320. https://doi.org/10.1179/009346908791071196
Lepère C (2014) Experimental and traceological approach for a technical interpretation of ceramic polished surfaces. J Archaeol Sci 46:144–155. https://doi.org/10.1016/j.jas.2014.03.010
Livingstone Smith A (2007) Chaine operatoire de la potterie: references ethnographiques, analyses et reconstitution. Musee Royal de l'Afrique Centrale, Tervuren.
Manem S (2020) Modeling the evolution of ceramic traditions through a phylogenetic analysis of the Chaînes Opératoires: the European Bronze Age as a case study. J Archaeol Method Theory 27:992–1039. https://doi.org/10.1007/s10816-019-09434-w
Manzaneda JC, Garcia XC, Roselló JG, Brun EP, Seguí MS (2018) Els processos de fabricació de ceràmiques a la Dou (Vall d'en Bas, la Garrotxa) durant el bronze final (1290–920 cal ANE). Primers Resultats Cypsela 21:43–66.
Mara H (2006) Documentation of rotationally symmetric archaeological finds by 3D shape estimation. Pattern Recognition and Image Processing Group Institute of Computer Aided Automation Vienna University of Technology.
Mara H (2009) Pottery plotted by laser – 3D acquisition for documentation and analysis of symmetry of ancient ceramics. In: Reindel M, Wagner G (eds) New technologies for archaeology, natural science in archaeology. Springer, Berlin Heidelberg, pp 379–390. https://doi.org/10.1007/978-3-540-87438-6_22
Martineau R (2000) Poterie, techniques et sociétés. Etudes analytiques et expérimentales à Chalain et Clairvaux (Jura), entre 3200 et 2900 av. J.-C. Université de Franche-Comté, Besançon.
Martineau R, Maigrot Y (2004) Les outils en os utilisés pour le façonnage des poteries néolithiques de la station 4 de Chalain (Jura, France). In: Bodu P, Constantin C (eds) Approches Fonctionnelles En Préhistoire, XXVe Congrès Préhistorique de France, Société Préhistorique Française, Paris (2004). Société Préhistorique française, Paris, pp 83–95.
Martineau R (2010) Brunissage, polissage et degrés de séchage: Un référentiel expérimental. Les Nouvelles De L'archéologie 119:13–19.
Martineau R (2013). Étude typologique, technologique et culturelle de la céramique. In: Le Petit Paulmy, Abilly (Indre-et-Loire). Un habitat du néolithique final de la région pressignienne. Tours : Fédération pour l'édition de la Revue archéologique du Centre de la France, pp. 255–323.
McKinney W (2010) Data structures for statistical computing in Python. In: Walt S, van der Millman J (eds) Proceedings of the 9th Python in Science Conference, pp 56–61. https://doi.org/10.25080/Majora-92bf1922-00a
Melis MG, Rosselló JG (2021) Chaînes opératoires et contacts techniques: l'analyse tracéologique du mobilier céramique du Chalcolithique de Sardaigne. In: Giligny F, Dolbunova E, Gomart L, Livingstone Smith A, Méry S (eds) Contribution of ceramic technological approaches to the anthropology and archaeology of pre- and protohistoric societies: Proceedings the XVIII UISPP World Congress (4–9 June 2018, Paris, France). Archaeopress Archaeology, Oxford, pp 50–65.
Monna F, Magail J, Rolland T, Navarro N, Wilczek J, Gantulga J-O, Esin Y, Granjon L, Allard A-C, Chateau-Smith C (2020) Machine learning for rapid mapping of archaeological structures made of dry stones – example of burial monuments from the Khirgisuur culture, Mongolia –. J Cult Herit 43:118–128. https://doi.org/10.1016/j.culher.2020.01.002
Navarro P, Cintas C, Lucena M, Fuertes JM, Delrieux C, Molinos M (2021) Learning feature representation of Iberian ceramics with automatic classification models. J Cult Herit 48:65–73. https://doi.org/10.1016/j.culher.2021.01.003
Nicodemus FE (1965) Directional reflectance and emissivity of an opaque surface. Appl Opt 4:767–775. https://doi.org/10.1364/AO.4.000767
Orton C, Tyers P, Vince A (1993) Pottery in archaeology. Cambridge University Press, Cambridge.
Pan SJ, Yang Q (2010) A survey on transfer learning. IEEE Trans Knowl Data Eng 22:1345–1359. https://doi.org/10.1109/TKDE.2009.191
Pétrequin P, Martineau R, Nowicki P, Gauthier E, Schaal C (2009) La poterie Hoguette de Choisey (Jura), les Champins. Observations techniques et insertion régionale. Bulletin De La Société Préhistorique Française 106:491–515.
Phong BT (1975) Illumination for computer generated pictures. Commun ACM 18:311–317.
Python Software Foundation (2021) Python language reference, version 3.8. http://www.python.org
R Core Team (2021) R: a language and environment for statistical computing. R Foundation for Statistical Computing, Vienna, Austria. https://www.R-project.org/
Renfrew C, Bahn P (2015) Archaeology. Theories, methods and practice (6th edition all in colour). Thames & Hudson, London.
Rice PM (2015) Pottery analysis: a sourcebook, 2nd edn. University of Chicago Press, Chicago, London.
Roux V (2017a) Ceramic manufacture: the chaîne opératoire approach, The Oxford handbook of archaeological ceramic analysis. Oxford University Press, Oxford, pp. 101–114. https://doi.org/10.1093/oxfordhb/9780199681532.013.8
Roux V (2017b) Smoothing and clay coating: reference collections for interpreting southern Levant Chalcolithic finishing techniques and surface treatments. The Arkeotek Journal. https://www.thearkeotekjournal.org
Roux V (2019) Ceramics and society: a technological approach to archaeological assemblages. Springer, Cham. https://doi.org/10.1007/978-3-030-03973-8
Ruder S (2017) An overview of gradient descent optimization algorithms. http://arxiv.org/abs/1609.04747
Russakovsky O, Deng J, Su H, Krause J, Satheesh S, Ma S, Huang Z, Karpathy A, Khosla A, Bernstein M, Berg AC, Fei-Fei L (2015) ImageNet large scale visual recognition challenge. http://arxiv.org/abs/1409.0575
Rye OS (1981) Pottery technology: principles and reconstruction. Taraxacum, Washington, D.C.
Santacreu DA (2014) Materiality, techniques and society in pottery production the technological study of archaeological ceramics through paste analysis. De Gruyter Open, Warsaw. https://doi.org/10.2478/9783110410204

Schlager S (2017) Chapter 9 - Morpho and Rvcg – shape analysis in R: R-packages for geometric morphometrics, shape analysis and surface manipulations. In: Zheng G, Li S, Szekely G (eds) Statistical shape and deformation analysis. Acad Press, pp 217–256. https://doi.org/10.1016/B978-0-12-810493-4.00011-0

Shepard AO (1956) Ceramics for the archaeologists. Carnegie Institution of Washington, Washington.

Skibo JM, Butts TC, Schiffer MB (1997) Ceramic surface treatment and abrasion resistance: an experimental study. J Archaeol Sci 24:311–317. https://doi.org/10.1006/jasc.1996.0115

Simonyan K, Zisserman A (2015) Very deep convolutional networks for large-scale image recognition. http://arxiv.org/abs/1409.1556

Stemp WJ (2014) A review of quantification of lithic use-wear using laser profilometry: a method based on metrology and fractal analysis. J Archaeol Sci 48:15–25. https://doi.org/10.1016/j.jas.2013.04.027

Stemp WJ, Chung S (2011) Discrimination of surface wear on obsidian tools using LSCM and RelA: pilot study results (area-scale analysis of obsidian tool surfaces). Scanning 33:279–293. https://doi.org/10.1002/sca.20250

Stemp WJ, Watson AS, Evans AA (2015) Surface analysis of stone and bone tools. Surf Topogr Metrol Prop 4:013001. https://doi.org/10.1088/2051-672X/4/1/013001

Tajbakhsh N, Shin JY, Gurudu SR, Hurst RT, Kendall CB, Gotway MB, Liang J (2016) Convolutional neural networks for medical image analysis: full training or fine tuning? IEEE Trans Med Imaging 35:1299–1312. https://doi.org/10.1109/TMI.2016.2535302

Thér R, Mangel T, Gregor M (2015) Život hrnčíře začíná v LT A. Výroba keramiky v době laténské na Chrudimsku. Filozofická fakulta UHK, Hradec Králové.

Thér R, Neumannová K (2012) Studium technologie úpravy povrchu keramiky kultury zvoncovitých pohárů prostřednictvím experimentu. Živá Archeologie REA 14:50–55.

Venclová N (1998) Mšecké Žehrovice in Bohemia: archaeological background to a Celtic hero, 3rd-2nd cent. B.C. Kronos B.Y. éditions, Sceaux.

Venclová N, Drda P, Michálek J, Militký J, Salač V, Sankot P, Vokolek V (2013). The prehistory of Bohemia 6. The Late Iron Age - The La Tène Period. Archeologický ústav AV ČR, Prague.

Wang H, He Z, Huang Y, Chen D, Zhou Z (2017) Bodhisattva head images modeling style recognition of Dazu Rock Carvings based on deep convolutional network. J Cult Herit 27:60–71. https://doi.org/10.1016/j.culher.2017.03.006

Wang X, Zhao Y, Pourpanah F (2020) Recent advances in deep learning. Int J Mach Learn Cybern 11:747–750. https://doi.org/10.1007/s13042-020-01096-5

Wilczek J, Monna F, Jébrane A, Labruère-Chazal C, Navarro N, Couette S, Chateau Smith C (2018) Computer-assisted orientation and drawing of archaeological pottery. J Comput Cult Herit 11:22. https://doi.org/10.1145/3230672

Wilczek J, Monna F, Navarro N, Chateau-Smith C (2021) A computer tool to identify best matches for pottery fragments. J Archaeol Sci Rep 37:102891. https://doi.org/10.1016/j.jasrep.2021.102891

Yosinski J, Clune J, Bengio Y, Lipson H (2014) How transferable are features in deep neural networks? In: NIPS'14: Proceedings of the 27th International Conference on Neural Information Processing Systems - Volume 2, pp 3320–3328. https://arxiv.org/abs/1411.1792

Zeiler MD (2012) ADADELTA: an adaptive learning rate method. http://arxiv.org/abs/1212.5701